

# Nanocrystallization of $\text{CaF}_2$ from $\text{Na}_2\text{O}/\text{K}_2\text{O}/\text{CaO}/\text{CaF}_2/\text{Al}_2\text{O}_3/\text{SiO}_2$ Glasses

Christian Rüssel

Otto-Schott-Institut, Universität Jena, Fraunhoferstrasse 6, 07743 Jena, Germany

Received July 1, 2005. Revised Manuscript Received September 19, 2005

In glasses with composition  $(100 - x)(9.9\text{Na}_2\text{O} \cdot 8.8\text{K}_2\text{O} \cdot 12.1\text{CaO} \cdot 6.6\text{Al}_2\text{O}_3 \cdot 62\text{SiO}_2) \cdot x\text{CaF}_2$  the glass-transition temperature decreases with increasing  $\text{CaF}_2$  concentration. Samples with  $x = 12.5$  were thermally treated at temperatures in the range from 520 to 560 °C for 1–80 h. This leads to crystallization of  $\text{CaF}_2$ . The quantity of crystalline  $\text{CaF}_2$  increases with increasing crystallization temperature, while the mean crystallite size remains constant. The glass-transition temperature of partially crystallized samples increases with increasing crystallization temperature and crystallization time and approaches a value equal to the temperature at which the samples were treated. This was explained by formation of a highly viscous layer enriched in  $\text{SiO}_2$  formed during crystallization, which acts as a diffusion barrier and hinders further crystal growth.

## 1. Introduction

Glass–ceramics containing metal fluoride crystals, such as alkaline-earth fluorides,  $(\text{Cd}, \text{Pb})\text{F}_2$  or  $\text{LaF}_3$  with crystallite sizes in the range from 5 to 100 nm are considered to be materials with high potential for numerous photonic applications.<sup>1–6</sup> Here, up-conversion glasses containing  $(\text{Ca}, \text{Pb})\text{F}_2$ <sup>5</sup> solid solutions doped with  $\text{YbF}_3$ <sup>2,4</sup> should be mentioned. In addition, glass–ceramics containing rare-earth-doped fluoride crystals are candidates for laser materials, combining the advantageous properties of glasses (ability to draw fibers) and crystals (large fluorescence lifetime), and considered for fiber amplifiers. For photonic applications the crystallite sizes must be smaller than one-half of the wavelength of the light used. Furthermore, the crystallite size distribution must be narrow in order to avoid light scattering, and the volume concentration should be at least some percent.

Usually the crystallization of glass is separated in two steps: nucleation and subsequent crystal growth. Nucleation rates usually exhibit a maximum at temperatures slightly above the glass-transition temperature. To determine nucleation rates (according to a method first described by Tamman<sup>7</sup>), a glass sample is brought to a temperature around or slightly above  $T_g$ , kept for a certain time, and then heated to a higher temperature at which the crystal growth velocity is large enough to enable the crystals to grow to an observable size. This procedure can only be applied because

at nucleation temperatures slight crystal growth also occurs. Otherwise the nuclei would dissolve again during heating<sup>8,9</sup> due to the increase of critical radius of the nuclei with increasing temperature (see, e.g., ref 10). Hence, if a sample is tempered at the nucleation temperature, nuclei are formed and simultaneously start to grow. In isochemical systems, i.e., those in which the crystalline phase formed possesses the same chemical composition as the glass it is crystallized from,<sup>11,12</sup> the crystal growth velocity does not depend on time. Usually glasses, glass–ceramics are prepared from, are not isochemical systems but 7–14-component systems (see, e.g., refs 13 and 14). Here, the chemical composition of the residual glassy matrix changes in the course of the nucleation and crystallization process, and hence the crystal growth velocity also changes with time. As recently described for the crystallization of  $\text{Fe}_3\text{O}_4$  from a  $\text{Na}_2\text{O}/\text{CaO}/\text{B}_2\text{O}_3/\text{Fe}_2\text{O}_3$  glass,<sup>15</sup> crystallization of a large volume concentration of nanocrystals may be enabled if the crystal growth velocity decreases in the course of the crystal growth, if near the crystals a diffusional barrier is formed.

Crystallization of fluoride-containing glasses has frequently been described in the literature<sup>16–20</sup> for silicate, phospho-

- (1) Fu, J.; Parker, J. M.; Flower, P. S.; Brown, R. M. *Mater. Res. Bull.* **2002**, 37, 1843.
- (2) Tanabe, S.; Hayashi, H.; Hanada, T.; Onodera, N. *Opt. Mater.* **2002**, 19, 343.
- (3) Mortier, M.; Monteville, A.; Partiche, G.; Mazé, G.; Auzel, F. *Opt. Mater.* **2001**, 16, 255.
- (4) Dejneka, M. J. *J. Non-Cryst. Solids* **1998**, 239, 149.
- (5) Wang, Y.; Ohwaki, J. *Appl. Phys. Lett.* **1993**, 63, 3268.
- (6) Kim, J. S.; Müller, M.; Seeber, W. *Glass Sci. Technol.* **2002**, 75 C2, 330.
- (7) Tamman, G. *Der Glaszustand*; Leopold Voss: Leipzig, Germany, 1933.

- (8) Davis, M. *Glastech. Ber. Glass Sci. Technol.* **2000**, 73 C1, 170.
- (9) Rüssel, C.; Keding, R. *J. Non-Cryst. Solids* **2003**, 328, 174.
- (10) Gutzow, I.; Schmelzer, J. *The vitreous state*; Springer: Berlin, Heidelberg, New York 1995.
- (11) Pewner, B. G.; Kluver, B. P. Proceedings of the XV International Congress Glass, Leningrad, Soviet Union, 1989; Vol. 26, p 277.
- (12) Kelton, K. F. *J. Non-Cryst. Solids* **2000**, 274, 147.
- (13) Beall, G. H. In *Advances in Nucleation and Crystallization in Glasses*; Hench, L. L., Freimann, S. W., Eds.; American Ceramic Society: Westerville, OH, 1972.
- (14) MacMillan, P. W. *Glass-Ceramics*; Academic Press: London, New York, San Francisco, 1979.
- (15) Woltz, S.; Rüssel, C. *J. Non-Cryst. Solids* **2004**, 337, 226.
- (16) Griggs, J. A.; Anusavice, K. J.; Mlechosky, J. J., Jr. *J. Mater. Sci.* **2002**, 37, 2017.
- (17) Deny, I. L.; Holloway, J. A. *J. Biomed. Mater. Res.* **2002**, 63, 146.
- (18) Stamboulis, A.; Hill, R. G.; Law, R. V.; Matsuya, S. *Phys. Chem. Glasses* **2004**, 45, 127.
- (19) Henry, J.; Hill, R. G. *J. Mater. Sci.* **2004**, 37, 1573.

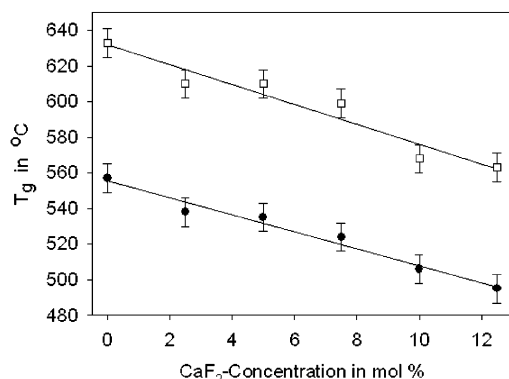


**Figure 1.** Glass-transition temperature,  $T_g$  (●), and dilatometric softening point (□) of glasses with mol % composition  $(100 - x)(9.9\text{Na}_2\text{O} \cdot 8.8\text{K}_2\text{O} \cdot 12.1\text{CaO} \cdot 6.6\text{Al}_2\text{O}_3 \cdot 62.6\text{SiO}_2) \cdot x\text{CaF}_2$  as a function of  $\text{CaF}_2$  concentration.

silicate, and borosilicate glasses. Here, the crystallization of fluoroapatite, fluoromica, and related structures as well as the general effect on nucleation is reported. In many systems addition of fluoride to the glass enhances nucleation.<sup>21,22</sup> This effect has also been described in the case of  $\text{CaF}_2$ . This paper presents a study on the crystallization of  $\text{CaF}_2$  from a glass in the system  $\text{Na}_2\text{O}/\text{K}_2\text{O}/\text{CaO}/\text{CaF}_2/\text{Al}_2\text{O}_3/\text{SiO}_2$ .

## 2. Experimental Section

Glasses with the composition  $(100 - x)(9.9\text{Na}_2\text{O} \cdot 8.8\text{K}_2\text{O} \cdot 12.1\text{CaO} \cdot 6.6\text{Al}_2\text{O}_3 \cdot 62.6\text{SiO}_2) \cdot x\text{CaF}_2$  were melted from reagent-grade  $\text{Na}_2\text{CO}_3$ ,  $\text{K}_2\text{CO}_3$ ,  $\text{CaCO}_3$ ,  $\text{CaF}_2$ ,  $\text{Al}(\text{OH})_3$ , and  $\text{SiO}_2$  (quartz) in batches of 200 g in a platinum crucible at 1480 °C. The melts were casted on a copper block and placed in a furnace preheated to 450 °C. Then the furnace was switched off, and the samples were allowed to cool.

The samples were thermally treated at temperatures in the range from 460 to 580 °C in a muffle furnace. Glasses and thermally treated samples were cut into pieces  $6 \times 6 \times 15 \text{ mm}^3$  and studied by a dilatometer (Netzsch 402 ES). From powdered thermally treated samples XRD patterns were recorded (Siemens D5000).

## 3. Results

The dilatometric curves recorded from the glassy samples showed glass-transition temperatures in the range from 495 to 557 °C. The dependence of  $T_g$  on  $\text{CaF}_2$  concentration is shown in Figure 1. Within the limits of error, the glass-transition temperature decreases linearly with increasing temperature. By analogy, the dilatometric softening temperature also decreases linearly with increasing  $\text{CaF}_2$  concentration. The curves run approximately parallel. The melted glasses were X-ray amorphous and visually transparent. X-ray diffraction patterns recorded from the tempered glasses with 12.5 mol %  $\text{CaF}_2$  exhibited lines attributable to  $\text{CaF}_2$  (JCPDS no. 35-0816). The tempered samples were studied by dilatometry in order to determine the glass-transition temperature of the residual glassy phase. In Figure 2 the determined glass-transition temperatures of samples thermally treated for 20 h at various temperatures in the range from 495 to 570 °C are shown. Tempering at 520 °C leads to an increase of the glass-transition temperature from 495 to 520

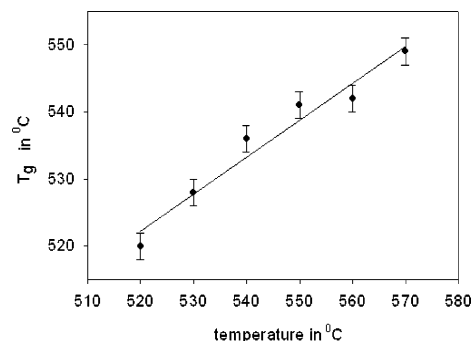


**Figure 2.** Glass-transition temperature,  $T_g$ , of glasses with mol % composition  $54.8\text{SiO}_2 \cdot 10.6\text{CaO} \cdot 12.5\text{CaF}_2 \cdot 8.6\text{Na}_2\text{O} \cdot 7.7\text{K}_2\text{O} \cdot 5.8\text{Al}_2\text{O}_3$  after heat treatment for 20 h as a function of the temperature of heat treatment.

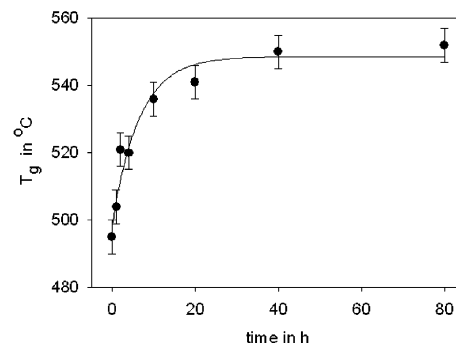


**Figure 3.** Glass-transition temperature,  $T_g$ , of a sample with mol % composition of  $54.8\text{SiO}_2 \cdot 10.6\text{CaO} \cdot 12.5\text{CaF}_2 \cdot 8.6\text{Na}_2\text{O} \cdot 7.7\text{K}_2\text{O} \cdot 5.8\text{Al}_2\text{O}_3$  after heat treatment at 550 °C as a function of the time of heat treatment.

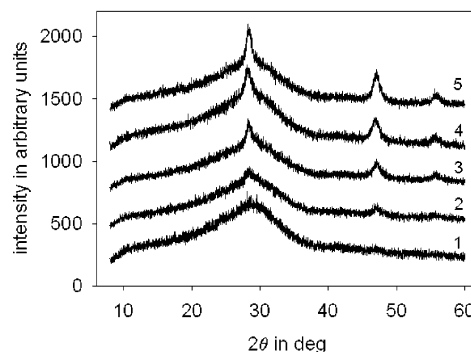


**Figure 4.** XRD patterns of samples heat treated at various temperatures for 20 h: (1) 520, (2) 530, (3) 540, (4) 550, and (5) 560 °C.

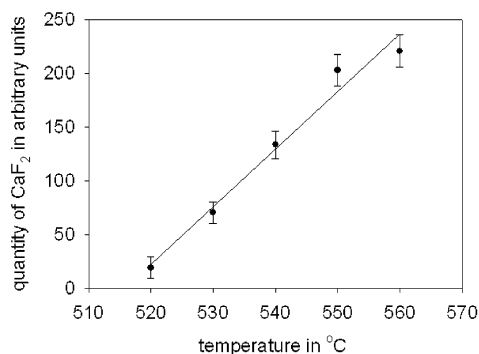
°C; tempering at higher temperature results in a further increase in the glass-transition temperature. After thermal treatment at 570 °C, the glass-transition temperature increases to a value of 549 °C. This value is nearly as large as the glass-transition temperature of the glass without  $\text{CaF}_2$ . The increase in the glass-transition temperature with thermal treatment temperature is linear within the limits of error. Figure 3 shows glass-transition temperatures of samples treated at 550 °C as a function of time. Within the first hour the glass-transition temperature increases from 495 to 521 °C. After tempering for 10 h a glass-transition temperature of 536 °C is reached. Thermal treatment for 20, 40, and 80 h results in glass-transition temperatures of 541, 550, and 552 °C, respectively.

Figure 4 presents XRD patterns of samples thermally treated at temperatures in the range from 520 to 560 °C and subsequently powdered. After thermal treatment at a temperature of 560 °C, distinct lines attributable to crystalline

(20) Douglas, R. W. *Br. J. Appl. Phys.* **1966**, *17*, 435.

(21) Assem, E. E. *J. Phys. D: Appl. Phys.* **2005**, *38*, 942.

(22) Hill, R.; Wood, D. J. *Mater. Sci. Mater. Med.* **1995**, *6*, 1573.



**Figure 5.** Quantity of CaF<sub>2</sub> formed (area under the XRD peak at 47°) as a function of the temperature the samples were treated at for 20 h.

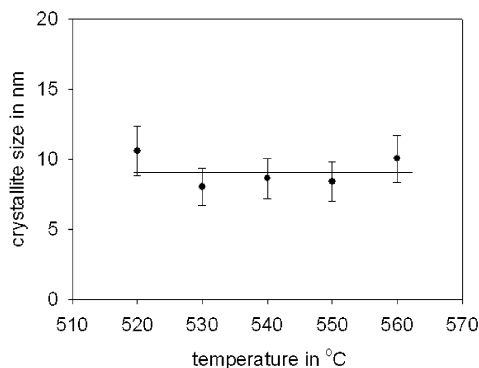


**Figure 6.** Mean crystallite sizes calculated by the Scherrer equation from XRD line broadening as a function of the temperature the samples were treated at for 20 h.

CaF<sub>2</sub> (JCPDS no. 35-0816) are seen at  $2\theta$  values of 28.3°, 47°, and 56°. The same lines, however, with smaller intensities are also observed in the XRD patterns of samples thermally treated at temperatures in the range from 530 to 550 °C. After tempering at 520 °C, only the XRD line at 47° is observed with marginal intensity. All lines are notably broadened. The XRD lines at around 47° were fitted by curves of Gaussian shape. The full-width at half-maximum (fwhm) as well as the area under the peak were calculated. Figure 5 presents the area under the peak which is a measure of the concentration of crystalline CaF<sub>2</sub>. It is seen that this concentration increases steadily and within the limits of error linearly with increasing thermal treatment temperature. In Figure 6 the mean crystallite size of the crystalline CaF<sub>2</sub> phase calculated by Scherrer's equation (see eq 1) is shown as a function of the temperature at which the sample was thermally treated. Here, it is assumed that XRD line broadening is not affected by stresses

$$d = \frac{G\lambda}{B \cos \theta} \quad (1)$$

with  $G = 0.899$  for a cubic system,  $\lambda$  = wavelength of X-ray radiation (Cu K $\alpha$  = 0.154 nm),  $B$  = fwhm, and  $\theta$  = Bragg angle of the XRD peak. The crystallite sizes are all in the range from 8 to 10.6 nm and within the limits of error do not depend on the thermal treatment temperature.

Figure 7 shows XRD patterns of samples tempered at 550 °C for different periods of time. In analogy to Figure 4, distinct lines attributed to CaF<sub>2</sub> are seen. After tempering for 4 h, a line of marginal intensity is visible at 47°. After tempering for at least 10 h, all three lines (28.3°, 47°, and

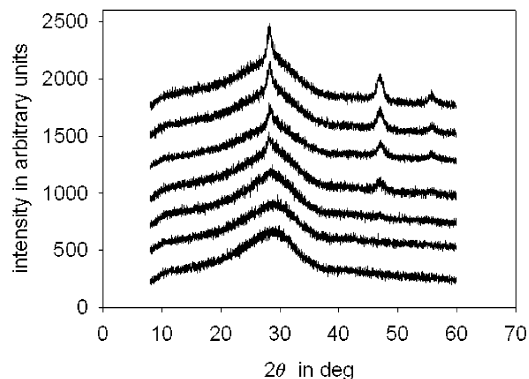


**Figure 7.** XRD patterns of samples heat treated at 550 °C for different periods of time: (1) 1, (2) 2, (3) 4, (4) 10, (5) 20, (6) 40, and (7) 80 h.

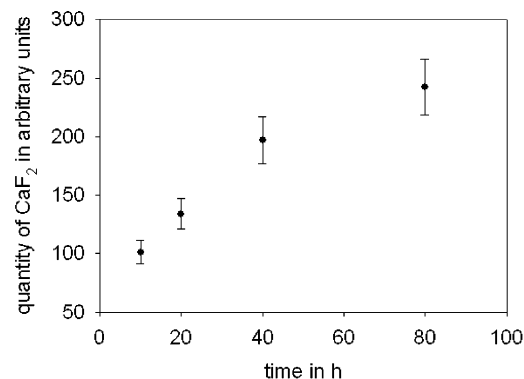


**Figure 8.** Quantity of CaF<sub>2</sub> formed (area under the XRD peak at 47°) as a function of the time the samples were heat treated at 550 °C.

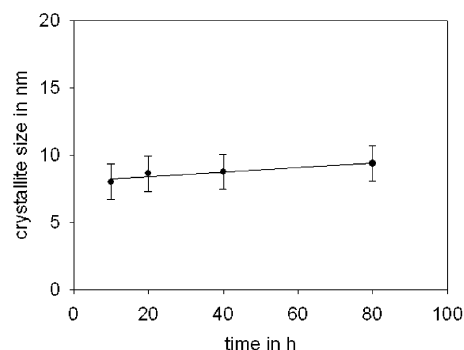


**Figure 9.** Mean crystallite sizes calculated by Scherrer's equation from XRD line broadening as a function of the time the samples were heat treated at 550 °C.

56°) can clearly be observed. In analogy to Figure 4, the XRD lines at around 47° were fitted by curves of Gaussian shape and the fwhm of the peak, the areas under the peak, and the mean crystallite sizes were calculated. The area under the peak, which is proportional to the concentration of formed crystalline CaF<sub>2</sub>, increases with increasing time of thermal treatment as shown in Figure 8. The mean crystallite size calculated by Scherrer's equation is shown in Figure 9. It is in the range from 8 to 9.4 nm and within the limits of error is not affected by the time of thermal treatment.

#### 4. Discussion

As shown in Figure 1, the glass-transition temperature as well as the dilatometric softening temperature decrease with increasing CaF<sub>2</sub> concentration. Hence, if CaF<sub>2</sub> is crystallized, the glass-transition temperature of the residual glass phase

increases due to a decrease of the  $\text{CaF}_2$  concentration. This is also observed in Figure 2. Here, increasing crystallization temperatures leads to increasing glass-transition temperatures.

As shown in Figures 4 and 7, the XRD lines are notably broadened. In principle, this may be due to two different effects. The first are small crystallites, the second is an inhomogeneous stress distribution in the crystals. Stresses in glass-ceramics are predominantly due to a mismatch in the thermal expansion coefficients of the glassy matrix and an inclusion. In the spherical case the stresses can be calculated by the Eshelby equation.<sup>23</sup>

The stresses inside the inclusion are isostatic and do not depend on the size of the crystals. Hence, they cannot be responsible for XRD line broadening, and it is justified to apply Scherrer's equation.

As shown in Figure 5, the quantity of crystalline  $\text{CaF}_2$  increases with increasing thermal treatment temperature. Hence, the increase of the glass-transition temperature and that of the quantity of crystalline  $\text{CaF}_2$  run parallel. Surprisingly, the mean size of the  $\text{CaF}_2$  crystals remains constant within the limits of error while increasing the crystallization temperature (see Figure 6). This means that the formed crystals do not grow further; only the number of crystals increases with increasing crystallization temperature. As shown in Figure 3 for a temperature of 550 °C, the glass-transition temperature increases with the time of thermal treatment and approaches a limiting value which within the limits of error is equal to the temperature at which the sample is thermally treated. The solid line drawn in Figure 3 is attributed to a fit according to eq 1

$$T_g = A + B(1 - e^{-Ct}) \quad (2)$$

with  $A = 499$  °C,  $B = 49.9$  °C, and  $C = 0.1525 \text{ h}^{-1}$ . Since the data in Figure 2 are attributed to a shorter time of thermal treatment (20 h), the limiting value is not yet reached while tempering at 550 °C. At lower temperatures of thermal treatment (520 and 530 °C) the glass-transition temperatures are already equal to the temperature at which the samples were treated after 20 h. It should be noted that crystallization of  $\text{CaF}_2$  cannot lead to a glass-transition temperature of the residual glass phase larger than 557 °C because this temperature is attributed to the glass without  $\text{CaF}_2$ .

The decrease in the glass-transition temperature with increasing time of thermal treatment runs parallel to the quantity of crystalline  $\text{CaF}_2$  formed (see Figure 8). However, the mean crystallite sizes shown in Figure 9 are the same within the limits of error, and hence, the crystals do not grow with time.

The crystallization behavior can be explained as follows: during nucleation of  $\text{CaF}_2$  and subsequent crystal growth, the melt near the nuclei is enriched in the other glass components.

In the present case, this layer is predominantly enriched in silica. This leads to an increase in viscosity near the nuclei. For a certain glass component the diffusivity in a first approximation should be proportional to the reciprocal viscosity and hence decrease in the course of the crystal-

lization process. Hence, a diffusional barrier is formed during nucleation and subsequent crystal growth which hinders further growth of the crystals. In the case of the system studied in this paper, the formed  $\text{CaF}_2$  crystals do not grow with time or if crystallization is carried out at higher temperatures. Formation of new nuclei should be inhibited near the already existing ones due to the larger viscosities in these regions. However, between the crystals nucleation continues. During further thermal treatment nucleation should occur in all regions of the sample of which the chemical composition is attributed to transformation temperatures that are below the temperature the sample is treated. Hence, the process continues until the viscosity of the whole residual glass melt possesses a value of  $10^{13}$  dPas. Then further nucleation gets more and more negligible and the crystallization process gets frozen in. At a given temperature the volume concentration of crystalline  $\text{CaF}_2$  approaches a constant value. If, however, a larger temperature is supplied, the volume concentration of crystalline  $\text{CaF}_2$  gets larger, since a viscosity of  $10^{13}$  dPas is attributed to a smaller  $\text{CaF}_2$  concentration in the residual glassy phase. The observation that the volume concentration of crystalline  $\text{CaF}_2$  increases with increasing thermal treatment temperature proves that  $\text{CaF}_2$  crystallization is limited by the nucleation kinetics. If it were due to the thermodynamics of the crystallization, most probably smaller temperatures should lead to larger quantities of crystalline  $\text{CaF}_2$  due to decreasing solubility of  $\text{CaF}_2$  in the melt. The crystallization of  $\text{CaF}_2$  from the melt composition considered is an example of a self-organized process. Both the volume concentration of crystalline  $\text{CaF}_2$  and the size of the formed crystals are controlled by the kinetics.

In principle, in nonisochemical systems crystal growth velocities should always depend on time since the chemical composition near the crystals changes during crystal growth. Here, two cases should be distinguished: (i) a phase enriched in network modifiers is crystallized. Then, as in the case of  $\text{CaF}_2$  crystallization, the viscosity near the crystal increases, and hence, the crystal growth velocity decelerates with time. In the second case (ii) a network former crystallizes. Then near the crystals the glassy phase is enriched in network modifiers. This leads to a decrease in viscosity near the crystal which should result in an increase in the crystal growth velocity.

Crystallization of components enriched in network modifiers hence generally should be advantageous in obtaining high volume concentrations of nanocrystallites. Precipitation of fluorides such as  $\text{CaF}_2$  or  $\text{LaF}_3$  further enables the incorporation of rare-earth metals into the lattice. This is especially valuable for the preparation of lasers, such as  $\text{YbF}_3$ -doped  $\text{CaF}_2$  embedded in a glassy matrix. In addition, up-conversion materials containing  $\text{Sm}^{3+}$ -doped  $(\text{Cd,Pb})\text{F}_2$  nanocrystals might be produced using the concept described above.

## Conclusion

From melts in the system  $\text{Na}_2\text{O}/\text{K}_2\text{O}/\text{CaO}/\text{CaF}_2/\text{Al}_2\text{O}_3/\text{SiO}_2$  crystalline  $\text{CaF}_2$  can be precipitated. The volume concentration of crystalline  $\text{CaF}_2$  increases with the thermal treatment temperature and also with time, approaching a constant value.

The mean crystallite sizes of CaF<sub>2</sub> are always in the range from 8 to 10.4 nm and do not get larger with time or when increasing the temperature (within the range studied). Since crystallization of CaF<sub>2</sub> leads to an increase in the viscosity near the crystals, a diffusional barrier around each crystal is formed which hinders further crystal growth. Between the

crystals nucleation proceeds until the whole residual glassy phase has a viscosity of 10<sup>13</sup> dPas. Then nucleation and crystallization are frozen in. The process is controlled by kinetics and is an example for self organization.

CM051430X